The Astrophysical Journal, 672:L49–L52, 2008 January 1

DUSTY DISKS AT THE BOTTOM OF THE INITIAL MASS FUNCTION

Alexander Scholz
SUPA, School of Physics and Astronomy, University of St. Andrews, North Haugh, St. Andrews, KY16 9SS, UK; as110@st-andrews.ac.uk
and
Ray Jayawardhana
Department of Astronomy and Astrophysics, University of Toronto, 50 St. George Street, Toronto, ON M5S 3H4, Canada; rayjay@astro.utoronto.ca
Received 2007 August 29; accepted 2007 November 9; published 2007 December 3

ABSTRACT

Isolated planetary-mass objects (IPMOs) have masses close to or below the deuterium-burning mass limit (∼15 $M_{\rm Jup}$)—at *the bottom of the stellar initial mass function*. We present an exploratory survey for disks in this mass regime, based on a dedicated observing campaign with the *Spitzer Space Telescope*. Our targets include the full sample of spectroscopically confirmed IPMOs in the σ Orionis cluster, a total of 18 sources. In the mass range 8–20 $M_{\rm Jup}$, we identify four objects with >3 σ color excess at a wavelength of 8.0 μm, interpreted as emission from dusty disks. We thus establish that a substantial fraction of IPMOs harbor disks with lifetimes of at least 2–4 Myr (the likely age of the cluster), indicating an origin from core collapse and fragmentation processes. The disk frequency in the IPMO sample is 29 $\pm^{16}_{13}$% at 8.0 μm, very similar to what has been found for stars and brown dwarfs (∼30%). The object S Ori 70, a candidate 3 $M_{\rm Jup}$ object in this cluster, shows IRAC colors in excess of the typical values for field T dwarfs (on a 2 σ level), possibly due to disk emission or low gravity. This is a new indication for youth and thus an extremely low mass for S Ori 70.

Subject headings: circumstellar matter — planetary systems — planetary systems: protoplanetary disks — stars: formation — stars: low-mass, brown dwarfs

1. INTRODUCTION

Over the past 5 years, it has been firmly established that the evolution of brown dwarfs from 1 to 10 Myr follows the blueprint known from T Tauri stars: they show evidence for ongoing gas accretion and outflows (e.g., Muzerolle et al. 2005; Mohanty et al. 2005) and harbor circumsubstellar disks with lifetimes of 5–10 Myr (e.g., Jayawardhana et al. 2003; Scholz et al. 2007), not vastly different from stars. This has often been interpreted as an indication for a common origin of stars and brown dwarfs—substellar objects as the natural extension of the stellar initial mass function (IMF) and the lowest-mass outcome of core collapse and fragmentation processes (see the review by Luhman et al. 2007 and references therein). At the same time, ongoing deep surveys have pushed the sensitivity limits down to masses below the deuterium-burning limit at ∼15 $M_{\rm Jup}$, finding evidence for a cluster population with masses comparable to giant planets (Zapatero Osorio et al. 2000; Lucas & Roche 2000). These objects *at the bottom of the IMF* are inconsistently called planemos, sub–brown dwarfs, cluster planets, or isolated planetary-mass objects in the literature; in the absence of a definite nomenclature, we will use the latter term (abbreviated IPMO) in the following.

The nature and origin of IPMOs have been debated intensely in recent years. Most of the problems raised in the discussions about the formation of brown dwarfs apply even more acutely to IPMOs (see the review by Whitworth et al. 2007). For example, it is under debate whether IPMOs can form directly from the collapse of ultra–low-mass cores; instead, they may be giant planets ejected from circumstellar disks or stellar embryos ejected from miniclusters or decaying multiple systems.

As of today, the observational constraints on the nature of IPMOs are very limited. Evidence for accretion or disks has been reported for a few young sources with masses around the deuterium-burning limit (Natta et al. 2002; Zapatero Osorio et al. 2002a; Luhman et al. 2005; Allers et al. 2006; Jayawardhana & Ivanov 2006). The next step is clearly to establish frequency and lifetimes of IPMO disks and to push the mass limits of disk surveys toward the least massive objects in star-forming regions. Here we present a *Spitzer* survey for disks around IPMOs in the σ Orionis cluster, which harbors the largest IPMO population identified thus far. With a well-explored stellar and brown dwarf population (Béjar et al. 2001; Caballero et al. 2007) and a likely age of 2–4 Myr (Zapatero Osorio et al. 2002c; Sherry et al. 2004), σ Ori is ideal for probing the disk frequency as a function of mass as well as the longevity of IPMO disks.

2. OBSERVATIONS AND PHOTOMETRY

As part of *Spitzer* program 30395 (PI: A. Scholz), we obtained deep Infrared Array Camera (IRAC) images in the four channels centered at 3.6, 4.5, 5.8, and 8.0 μm for 18 objects in the σ Ori cluster with estimated masses below 20 $M_{\rm Jup}$. All targets have been identified initially in deep photometric surveys (Zapatero Osorio et al. 2000, 2002b; Caballero et al. 2007). With one exception, all objects have been confirmed as likely ultra–low-mass young cluster members with low-resolution spectroscopy; however, given the low signal-to-noise ratio of the spectra, this should not be taken as a definite membership confirmation. In particular, the membership is under debate for S Ori 70 (see § 4) and S Ori 47 (McGovern et al. 2004). See Table 1 for more information and references for the target properties.

The objects, covered with 13 IRAC fields, were observed in a 12 position dither pattern with the medium scale and 100 s integration time per position. In total, this gives 1200 s on-source time per target in each channel, a factor of 10 deeper (in signal-to-noise ratio) than the GTO/IRAC survey of this cluster (program 37, PI: G. Fazio; see Hernández et al. 2007). For the analysis, we made use of the post–Best Calibrated Data (BCD) mosaics provided by the IRAC pipeline version S15.3.0. While parts of some images are affected by saturation effects and stray light from bright stars, in the regions where our targets are located, the image quality is in most cases excellent.

All objects are detected in channels 1 and 2; two are not detected in channel 3, while four are invisible in channel 4. For the object S Ori 54, we used the publicly available GTO survey

TABLE 1
Targets and *Spitzer* Photometry in the σ Ori Cluster

Name	Spectral Type[a]	I[b] (mag)	$I-J$[b] (mag)	3.6 μ (mag)	4.5 μ (mag)	5.8 μ (mag)	8.0 μ (mag)	Comment
S Ori 71	L0	20.02	2.88	15.24 ± 0.06	14.83 ± 0.06	14.29 ± 0.08	13.84 ± 0.13	Disk
S Ori 47	L1.5	20.53	3.15	14.87 ± 0.06	14.91 ± 0.06	14.77 ± 0.11	14.90 ± 0.33	
S Ori 50	M9	20.66	3.12	15.66 ± 0.06	15.64 ± 0.06	15.95 ± 0.30	15.63 ± 0.70	
S Ori 51	M9	20.71	3.50	15.42 ± 0.06	15.30 ± 0.06	15.19 ± 0.15	15.35 ± 0.51	
S Ori 53	M9	21.17	3.28	16.02 ± 0.06	15.84 ± 0.06	16.69 ± 0.63	15.47 ± 0.58	
S Ori 54	M9.5	21.29	3.30	15.8 ± 0.1[c]	∼15.6[c,d]	∼15.3[d]	>15.1	
S Ori 55	M9	21.32	3.10	16.41 ± 0.06	16.19 ± 0.07	16.18 ± 0.37	15.83 ± 0.90	
S Ori 56	L0.5	21.74	3.30	16.12 ± 0.06	15.79 ± 0.06	15.62 ± 0.22	15.27 ± 0.48	
S Ori 58	L0	21.90	3.30	16.43 ± 0.06	16.19 ± 0.07	15.52 ± 0.20	∼16.7[d]	Disk?
S Ori J053949.5−023130	N.A.	22.04	3.15	16.49 ± 0.06	16.32 ± 0.07	15.73 ± 0.25	15.05 ± 0.38	Disk
S Ori 60	L2	22.75	3.58	16.61 ± 0.06	16.34 ± 0.07	15.34 ± 0.18	14.34 ± 0.20	Disk
S Ori 62	L2	23.03	3.59	16.50 ± 0.06	16.36 ± 0.07	16.02 ± 0.32	∼17.2[d]	
S Ori 65	L3.5	23.23	3.33	16.72 ± 0.07	16.60 ± 0.08	16.05 ± 0.33	15.05 ± 0.38	Disk
S Ori 66	L3.5	23.23	3.40	17.41 ± 0.1[c]	16.87 ± 0.1[c]	16.05 ± 0.33	15.53 ± 0.62	Disk?
S Ori 67	L5	23.40	3.49	17.75 ± 0.10	17.64 ± 0.16	∼17.6[d]	>15.1	
S Ori 68	L5	23.77	3.59	16.49 ± 0.06	16.39 ± 0.07	>16.2	>15.1	
S Ori 69	T0	23.89	3.64	16.87 ± 0.07	17.14 ± 0.12	>16.2	>15.1	
S Ori 70	T	25.03	4.75	18.83 ± 0.25	17.14 ± 0.11	∼17.2[d]	>15.1	

[a] Spectral types from Martín et al. 2001; Barrado y Navascués et al. 2001; Zapatero Osorio et al. 2002b; Barrado y Navascués et al. 2002.
[b] Optical/NIR photometry from Zapatero Osorio et al. 2000, 2002b; Caballero et al. 2007.
[c] Fluxes measured in GTO images.
[d] Uncertainty is approximately ±0.5 mag.

data to measure fluxes in channels 1 and 2, because in our deep images the source is "drowned" in the emission from a nearby extended object and two nearby point sources (all within 8″). The object S Ori 66 is located on a dark row in our IRAC1 and 2 images; again we obtained fluxes for this object from the GTO data.

Fluxes were measured by aperture photometry with relatively small apertures (3–5 pixels) using routines in *daophot*. For all objects, the aperture is free from visible neighbors. Aperture corrections were applied, as given in the IRAC data handbook (ver. 3.0). Fluxes were converted to magnitudes using the recommended zero points quoted in the data handbook. All IRAC magnitudes for the IPMOs are reported in Table 1.

The dominant error source is background uncertainty. To get a realistic estimate, we measured the flux in empty regions in our images using the same method as for the targets (>50 measurements in IRAC1 and 2, >80 in IRAC3 and 4). As expected, these values scatter around zero; their rms defines the uncertainty in flux measurements due to background noise and small-scale fluctuations and thus gives a conservative estimate on the photometric error for faint sources. We obtain 1.8, 2.2, 12.7, and 20.3 μJy in channels 1–4, respectively. Note that these values do not correspond to the detection limits, which are better defined using the peak count rate of the point-spread function in comparison with the background scatter in the sky annulus. All objects for which fluxes are given in the table are detected with a signal-to-noise ratio of at least 4.

The total errors quoted in Table 1 are composed of photometric errors and systematics. The latter ones are the combination of uncertainties in calibration (5%) and aperture correction (1%–2%, from the IRAC data handbook). No color correction was carried out; instead we added a small contribution (0%–2%) to the error budget. The upper limits quoted in Table 1 correspond to 3 times the photometric errors. In channels 1 and 2, our fluxes are in excellent agreement (within 0.2 mag) with the values reported recently by Zapatero Osorio et al. (2007) for a subsample of our targets. In channels 3 and 4, the magnitude differences between our work and that of Zapatero Osorio et al. (2007) typically remain within 0.6 mag, still within the 1 σ error bars. We note, however, that in these two bands our fluxes are in most cases substantially lower than the values given by Zapatero Osorio et al. (2007).

3. DISK FREQUENCY IN THE PLANETARY-MASS REGIME

We search for mid-infrared emission from dusty disks in our sample by comparing the measured IRAC colors with published values for (diskless) field objects in the same $T_{\rm eff}$ range (Patten et al. 2006). The main discriminators to distinguish between the photospheric contribution and the disk excess are the fluxes in IRAC channels 3 and 4; at shorter wavelengths the contrast between the photosphere and a possible disk is difficult to detect. In Figure 1 we plot IRAC colors (I1−I4 and I1−I3) for all targets (except S Ori 70; see § 4). As abscissa in these plots we use the $I-J$ color, which can be assumed to be purely photometric and thus represents a proxy for $T_{\rm eff}$, which in turn correlates with mass for coeval objects. The plot covers a mass range from ∼20 to ∼8 $M_{\rm Jup}$. IPMOs are shown as crosses; the solid lines are linear fits to the colors of the field objects and thus delineate the photospheric level in these figures.

As can be seen in this plot, the majority of the IPMOs have IRAC colors indistinguishable from the photospheric values and can thus be assumed to have either no disk or only small amounts of dust in the inner disk. Sources that lack excess in our data include S Ori 54, S Ori 55, and S Ori 56, for which Zapatero Osorio et al. (2007) reported disk detections based on the shallow GTO IRAC images. If we use the IRAC3 color as disk criterion (*upper panel*), we find that four objects—S Ori 71, S Ori 60, S Ori 66, and S Ori 58—show excess at the 3 σ level, i.e., 4 out of 17 or 24 $\pm^{13}_{11}$%. Since disk excesses may appear only beyond 5.8 μm, the result from IRAC3 should be considered to be a lower limit.

Based on the IRAC4 color (*lower panel*), we find four sources—S Ori 71, S Ori J053949.5−023130, S Ori 60, and S Ori 65—with >3 σ color excesses, which we consider to be primary disk detections.[1] In all four cases the excess increases significantly in IRAC channel 4 compared with channel 3, in-

[1] The object S Ori 66, albeit having a high I1−I4 color of 1.88 mag, is not counted here, because it has a large error bar in IRAC4. A particular case may be the object S Ori 58, which does have excess in IRAC3 but appears below the photospheric level in IRAC4. This object has been identified to have a disk by Zapatero Osorio et al. (2007) based on an IRAC4 flux that is significantly higher than our measurement. Possible reasons for these ambiguous findings include significant background variations in that area, which might hamper accurate photometry.

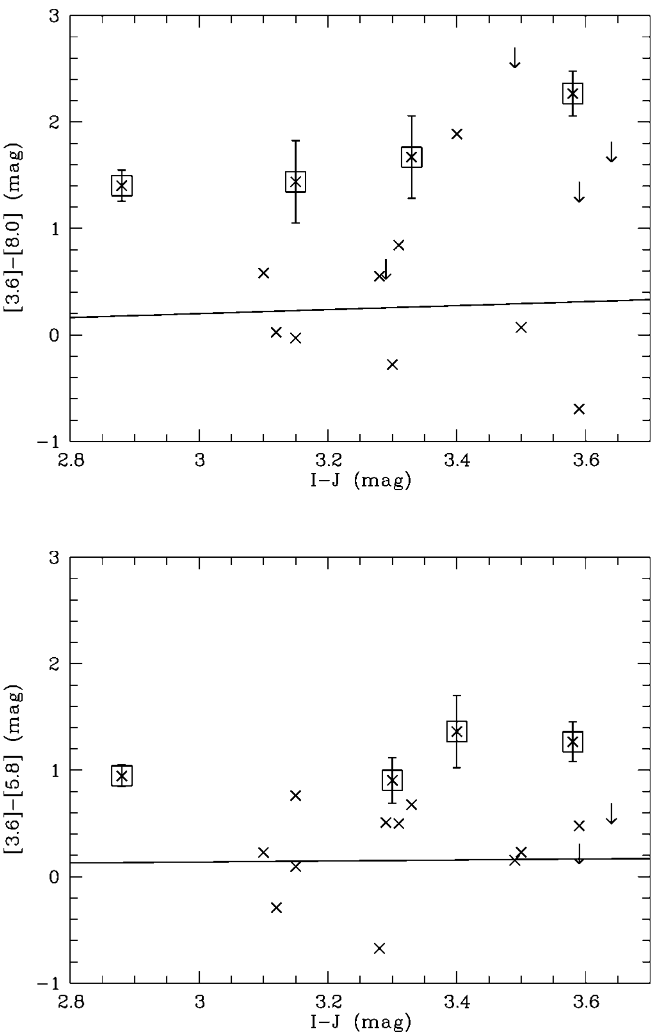

FIG. 1.—IRAC colors for IPMOs in σ Ori (*crosses*) in comparison with field M/L dwarfs (Patten et al. 2006; *solid line*). Objects with >3 σ excess with respect to the field dwarfs are marked with squares.

dicating rising flux levels toward longer wavelengths, a clear signature of disk emission. With the exception of S Ori 65, these objects have been published previously as disk-bearing very low mass sources (Caballero et al. 2007; Zapatero Osorio et al. 2007). This gives a disk fraction of 4 out of 14 or 29 $\pm^{16}_{13}$%. Here we do not count the three objects with upper limits well above the photospheric level, for which we cannot decide if they have disk excess or not. Disk frequencies derived from IRAC3 and IRAC4 are thus consistent; since the value determined from IRAC4 is likely to be more robust, we put more emphasis on this result. We note that the disk fraction in our sample might still be somewhat higher than given here, due to the combined effects of photometric uncertainties and contaminating field objects (see the discussion in Caballero et al. 2007).

We now compare our disk detection rate with previous results for more massive objects in σ Ori, as given by Hernández et al. (2007) based on IRAC data: 15% for HAeBe stars, 27% for intermediate-mass T Tauri stars, 36% for T Tauri stars, and 33% for brown dwarfs. The value for brown dwarfs is in agreement with the disk fraction of 33% derived by Jayawardhana et al. (2003) from ground-based L''-band imaging. A higher brown dwarf disk fraction of 47% has been published by Caballero et al. (2007). For the IPMO range (objects with $M \lesssim 20\ M_{\rm Jup}$), we now derive a disk fraction of 29%, which is compatible with the values for T Tauri stars and brown dwarfs within the 1 σ uncertainties. We do not see a trend to higher disk frequencies in the IPMO range, as claimed by Zapatero Osorio et al. (2007); instead the evidence points to comparable disk fractions for planetary-mass objects, brown dwarfs, and T Tauri stars, i.e., over more than 2 orders of magnitude in object mass (0.008–2 $M_\odot$).

We note that two of the objects with disk excess, S Ori 66 and S Ori 71, stand out from the rest of the sample, as they show excessively strong Hα emission with equivalent widths of ∼100 and ∼700 Å, respectively (Barrado y Navascués et al. 2001, 2002). This indicates that the presence of a dusty disks is likely accompanied by ongoing gas accretion, causing intense Hα emission, as observed in T Tauri stars and brown dwarfs.

4. THE CASE OF S ORI 70

The faintest target in our sample, S Ori 70, has been reported originally as a ∼3 $M_{\rm Jup}$ IPMO with tentative spectral type T5.5 (Zapatero Osorio et al. 2002b) . If confirmed, it would be the lowest-mass free-floating object found to date. Its mass would put it close to or even beyond the predicted opacity limit for fragmentation (see Bonnell et al. 2007 and references therein) and thus poses a challenge for star formation theory. However, Burgasser et al. (2004) have questioned the cluster membership (and thus the extremely low mass) of S Ori 70 and argue that its near-infrared spectrum is perfectly consistent with a foreground dwarf with spectral type ∼T6–7. In response, Martín (2004) reiterated the claim for cluster membership and youth mainly based on the $H-K$ color of S Ori 70, which is unusually high for a T dwarf and is interpreted as evidence for low surface gravity. To date, the nature of this object remains unclear. Our deep IRAC images now allow a reinvestigation of the issue.

S Ori 70 is clearly detected in IRAC channels 1 and 2. In addition, it is detected in IRAC3, with a ∼4 σ significance (peak count rate over background noise). The IRAC3 flux uncertainty has been derived on the basis of the very fact that the object is just detected—if it were $\gtrsim$25% fainter than the estimated 17.2 mag, we would not be able to see it. In Figure 2 we plot its IRAC colors versus spectral type in comparison with measurements for field T dwarfs, taken from Patten et al. (2006). S Ori 70 is tentatively plotted as spectral type T6 (average of the two available literature estimates).

As can be seen in this figure, the field T dwarfs form a clear sequence, whereas S Ori 70 stands out: in both IRAC colors, it appears to have some excess. Compared with the mean trend for the field T dwarfs, the significance of this excess is ∼2 σ in both IRAC2 and IRAC3. This excess cannot be accounted for by uncertainties in the spectral type, since the 3.6–5.8 μm color saturates in the late-T dwarf regime and reaches maximum values of ∼1.2—compared with 1.6 for S Ori 70. It should also be pointed out that S Ori 70 is brighter than the more massive L5 dwarf S Ori 67 in IRAC2 and 3, again indicating an unusual spectral energy distribution for this object.

There are two possible origins for a mid-infrared color excess in S Ori 70: (*a*) As reported by Leggett et al. (2007), gravity affects the near/mid-infrared colors of mid/late-T dwarfs in the sense that it can produce a significant excess at 2–6 μm for low-gravity objects. (*b*) Similarly to the L-type IPMOs in σ Ori, S Ori 70 might harbor a dusty disk, which produces the IRAC excess. Both possibilities provide additional evidence for youth, and thus the mid-infrared excess bolsters the claim that it is the lowest-mass free-floating object identified thus far. In case the mid-infrared excess is due to a dusty disk, this can be interpreted as evidence for a starlike infancy. While the uncertainties in the IRAC fluxes are too large at this stage for a definitive answer, these new findings certainly motivate further follow-up work on this target.

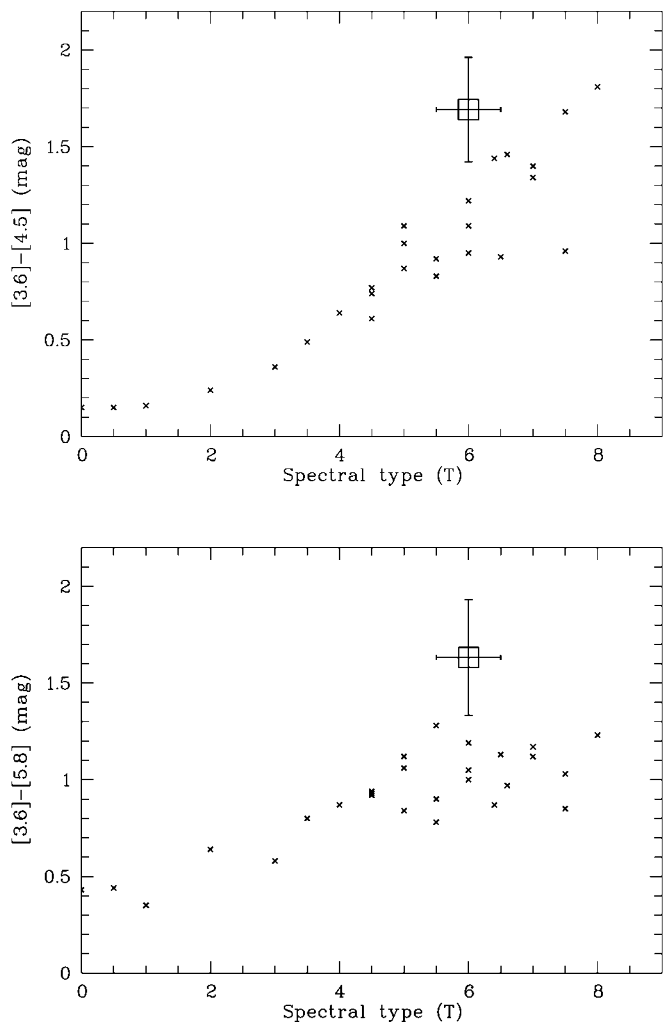

FIG. 2.—The IRAC colors of S Ori 70 (*square*) compared with field T dwarfs (Patten et al. 2006; *small crosses*).

5. SUMMARY

We have conducted a disk survey for isolated planetary-mass objects, based on deep observations with the *Spitzer Space Telescope*. Our targets comprise the full sample of spectroscopically confirmed IPMOs in the σ Orionis cluster. As a pioneering study, the results presented here are not intended to be the last word on the subject. Instead, we intend this Letter to serve as an important step toward a more profound understanding of the nature and origin of the lowest-mass objects found in isolation.

A substantial fraction of our targets exhibits mid-infrared excess emission indicative for the existence of a dusty disk. From our IRAC data, we derive a disk fraction of $29 \pm^{16}_{13}\%$ (4/14) at 8.0 μm. A similar value is found at 5.8 μm. These results are fully consistent with the disk frequencies derived for T Tauri stars and brown dwarfs in the same cluster. The detection of dusty disks around IPMOs in σ Ori is another firm evidence for their nature as lowest-mass members of this young cluster. The finding clearly establishes that objects at the bottom of the IMF can harbor dusty disks with lifetimes of at least 2–4 Myr, the most likely age of the σ Ori. Thus, our results fit into previous claims for a T Tauri–like phase in the planetary-mass regime (Natta et al. 2002; Luhman et al. 2005; Allers et al. 2006; Jayawardhana & Ivanov 2006). Disk fractions and thus lifetimes are similar for objects spanning more 2 orders of magnitude in mass (0.008–2 $M_{\odot}$), possibly indicating that stars, brown dwarfs, and IPMOs share a common origin. Star formation theory thus has to account for a number of objects with masses below the deuterium-burning limit.

Our sample includes S Ori 70, the faintest candidate member so far in σ Ori, which is detected in our IRAC images from 3.6 to 5.8 μm. Compared with field T dwarfs, the source stands out on the basis of the IRAC colors, with excesses at 4.5 and 5.8 μm at a 2 σ level. This may be an indication for youth and possibly disk occurrence for an object with an estimated mass of 3 $M_{\rm Jup}$ (Zapatero Osorio et al. 2002b). Uncertainties are large, though, meaning that this should be seen as motivation for further follow-up rather than a definite confirmation of the "cluster planet" nature of this object.

This work was supported in part by an NSERC grant to R. J.

REFERENCES

Allers, K. N., Kessler-Silacci, J. E., Cieza, L. A., & Jaffe, D. T. 2006, ApJ, 644, 364
Barrado y Navascués, D., Zapatero Osorio, M. R., Béjar, V. J. S., Rebolo, R., Martín, E. L., Mundt, R., & Bailer-Jones, C. A. L. 2001, A&A, 377, L9
Barrado y Navascués, D., Zapatero Osorio, M. R., Martín, E. L., Béjar, V. J. S., Rebolo, R., & Mundt, R. 2002, A&A, 393, L85
Béjar, V. J. S., et al. 2001, ApJ, 556, 830
Bonnell, I. A., Larson, R. B., & Zinnecker, H. 2007, in Protostars and Planets V, ed. B. Reipurth, D. Jewitt, & K. Keil (Tucson: Univ. Arizona Press), 149
Burgasser, A. J., Kirkpatrick, J. D., McGovern, M. R., McLean, I. S., Prato, L., & Reid, I. N. 2004, ApJ, 604, 827
Caballero, J. A., et al. 2007, A&A, 470, 903
Hernández, J., et al. 2007, ApJ, 662, 1067
Jayawardhana, R., Ardila, D. R., Stelzer, B., & Haisch, K. E. 2003, AJ, 126, 1515
Jayawardhana, R., & Ivanov, V. D. 2006, ApJ, 647, L167
Leggett, S. K., Saumon, D., Marley, M. S., Geballe, T. R., Golimowski, D. A., Stephens, D., & Fan, X. 2007, ApJ, 655, 1079
Lucas, P. W., & Roche, P. F. 2000, MNRAS, 314, 858
Luhman, K. L., Adame, L., D'Alessio, P., Calvet, N., Hartmann, L., Megeath, S. T., & Fazio, G. G. 2005, ApJ, 635, L93
Luhman, K. L., Joergens, V., Lada, C., Muzerolle, J., Pascucci, I., & White, R. 2007, in Protostars and Planets V, ed. B. Reipurth, D. Jewitt, & K. Keil (Tucson: Univ. Arizona Press), 443
Martín, E. L. 2004, eprint (ArXiv:astro-ph/0410678)
Martín, E. L., Zapatero Osorio, M. R., Barrado y Navascués, D., Béjar, V. J. S., & Rebolo, R. 2001, ApJ, 558, L117
McGovern, M. R., Kirkpatrick, J. D., McLean, I. S., Burgasser, A. J., Prato, L., & Lowrance, P. J. 2004, ApJ, 600, 1020
Mohanty, S., Jayawardhana, R., & Basri, G. 2005, ApJ, 626, 498
Muzerolle, J., Luhman, K. L., Briceño, C., Hartmann, L., & Calvet, N. 2005, ApJ, 625, 906
Natta, A., Testi, L., Comerón, F., Oliva, E., D'Antona, F., Baffa, C., Comoretto, G., & Gennari, S. 2002, A&A, 393, 597
Patten, B. M., et al. 2006, ApJ, 651, 502
Scholz, A., Jayawardhana, R., Wood, K., Meeus, G., Stelzer, B., Walker, C., & O'Sullivan, M. 2007, ApJ, 660, 1517
Sherry, W. H., Walter, F. M., & Wolk, S. J. 2004, AJ, 128, 2316
Whitworth, A., Bate, M. R., Nordlund, Å., Reipurth, B., & Zinnecker, H. 2007, in Protostars and Planets V, ed. B. Reipurth, D. Jewitt, & K. Keil (Tucson: Univ. Arizona Press), 459
Zapatero Osorio, M. R., Béjar, V. J. S., Martín, E. L., Barrado y Navascués, D., & Rebolo, R. 2002a, ApJ, 569, L99
Zapatero Osorio, M. R., Béjar, V. J. S., Martín, E. L., Rebolo, R., Barrado y Navascués, D., Bailer-Jones, C. A. L., & Mundt, R. 2000, Science, 290, 103
Zapatero Osorio, M. R., Béjar, V. J. S., Martín, E. L., Rebolo, R., Barrado y Navascués, D., Mundt, R., Eislöffel, J., & Caballero, J. A. 2002b, ApJ, 578, 536
Zapatero Osorio, M. R., Béjar, V. J. S., Pavlenko, Y., Rebolo, R., Allende Prieto, C., Martín, E. L., & García López, R. J. 2002c, A&A, 384, 937
Zapatero Osorio, M. R., et al. 2007, A&A, 472, L9